* * *

The review of publications on dependence of dendrite arm spacing microstructure of carbon and low-alloy steels from their chemical composition testifies that evaluation of this effect obtained by experiments and presented by statistical models, is characterized by significant differences in mathematical form, as well as the sign and magnitude of the regression coefficients which evaluate the contribution of different components of steel. As a result, the collection of presented models has contradictory character, that does not allow its unambiguous usage for governing of dendrite arm spacing by modification of steel composition and varying the determining factors.

Improvement of the quality of statistical models (the exception of insignificant effects caused by certain components, elimination the correlation distortion, etc.) and ensuring of their adequacy can be achieved via reasonable unification the description of the experimental data on the basis of a polynomial form of the concentration term of the regression equation, obtained by means of orthogonal experimental design .

Computer-aided analysis of forming dendritic structure on the base of calculation of non-equilibrium solidification, taking into account the changes in the composition of the liquid phase and the evolution of dendrite arm spacing, allows quantitative evaluation of the role of physical-chemical and thermal-physical factors in the development of coalescence of secondary arms. It is established the reduction of the secondary dendrite spacing in carbon and low alloy steels with growth of carbon, silicon, manganese, chromium, and nickel content, as well as the increase in the proportion of austenite during solidification, due to the suppression of diffusion transport of components during coalescence of dendritic branches.

REFERENCES (Part 2)

36. *Golod V. M., Emelyanov K. I., Orlova I. G.* Prediction of dendritic micro-heterogeneity of cast steel: review of models and computer-aided analysis of problems. (Part 1. Models based on thermal-physical parameters). — CIS Iron and Steel Review. 2013. pp. 21–28.
37. *Taha M. A.* Some observations of dendritic morphology and dendrite arm spacing. Metal Science. 1979. No. 1. pp. 9–12.
38. *Guo W., Zhu M.* Characteristic parameters for dendritic microstructure of solidification during slab continuous casting. Journal of Iron and Steel Research, International. 2009. Vol. 16, No. 1. pp. 17–21.
39. *Han Q., Hu H., Zhong X.* Models for the isothermal coarsening of secondary dendrite arms in multicomponent alloys. Metallurgical and Materials Transactions. 1997. Vol. 28B, No. 6. pp. 1185–1187.
40. *Miettinen J.* Thermodynamic-kinetic simulation of constrained dendrite growth in steel. Metallurgical and Materials Transactions. 2000. Vol. 31B, No. 2. pp. 365–379.
41. *Nalimov V. V., Chernova A. A.* Statisticheskie metody planirovaniya ekstremalnykh eksperimentov (Statistic methods of design of extremal experiments). Moscow : Nauka, 1965. 340 p.
42. *Golod V. M., Emelyanov K. I., Orlova I. G.* Dendritnaya mikroneodnorodnost stalnykh otlivok: obzor issledovaniy i kompyuternyy analiz. Sbornik "Liteynoe proizvodstvo segodnya i zavtra". Trudy 9 Vserossiyskoy nauchno-tekhnicheskoy konferentsii (Dendritic microinhomogeneity of steel founding: review of researches and computer analysis. Collection "Foundry today and tomorrow". Proceedings of the 9-th All-Russian scientific and technical conference). Saint Petersburg, Publishing House of Polytechnical University, 2012. pp. 436–455.

Prediction of dendritic micro-heterogeneity of cast steel: review of models and computer-aided analysis of problems (Part 3. Local structural and chemical heterogeneity)

***V. M. Golod*[1], *K. I. Emelyanov*[1], *I. G. Orlova*[1]**
[1] *Saint-Petersburg State Polytechnic University (St. Petersburg, Russia)*
E-mail: cheshire@front.ru

In the third part of the review it is noted that the number of publications devoted to the problem of heterogeneity of dendritic structure on the microscale, is very little. They have no significant results and methods that can reveal the basic laws of the evolutionary transformation of secondary dendritic branches from the moment of their inception to the final state. The coalescence models of dendritic branches are traditionally used to calculate the average value of the secondary dendrite spacing. The experimental data evaluates considerable scatter of dendrite arm spacing relative to the average values with a coefficient of variation V = 0.20–0.25.

Using a Monte Carlo simulation, it was implemented the solution of formation of an array of data, according to

the final distribution of secondary dendrite arm spacing based on local system for the coalescence of neighboring secondary branches. Computer calculations of coalescence for the local systems were done repeatedly by varying their initial morphology randomly. This leads to the different character of evolution with the activation of various competing mechanisms for individual local systems. The multiple implementations of this procedure for a large number of local systems lead to the formation of data that describe the resulting dendritic structure with its statistical parameters — the mean, standard deviation and probability density distribution (frequency) in the form of a histogram.

The simulation results are used to assess the contribution of different mechanisms of coalescence and are in good agreement with experimental data in predicting a broad spectrum of values dendrite arm spacing.

The radical increase in the accuracy of forecasting and analysis of the conditions of formation of the dendritic structure can be achieved through the development and application of computer models of non-equilibrium solidification of ingots and castings that are based on the use of thermal-physical and physical-chemical characteristics of the alloys, determined by their thermodynamic simulation, taking into account the rate of convective heat transfer at the front formation of dendrites. At the analysis and synthesis of empirical information on the dendritic structure for the objective evaluation of the quality of initial information and to ensure the adequacy of the resulting models requires the use of modern statistical analysis of experimental data. It is advisable to unify the description of the experimental data on the basis of a polynomial form of the concentration factor of the regression equation.

Key words: *dendritic structure, dendrite arm spacing, mechanisms of diffusion coalescence, Monte-Carlo method, computer simulations, non-equilibrium crystallization.*

Setting of the problem. Prediction of microstructure of alloys is one of the priority tasks for analysis and computer-aided simulation of their crystallization. The massif of publications presented in the previous part of this review is characterized by practically complete lack of any data about the features of averaging of experimental parameters. This averaging was applied to the pilot data, suggested for discussion as figures and generalized statistical models. Those publications reflected the data only about average values of secondary dendritic arm spacing $(\lambda_2)_{av}$, obtained on the base of statistical analysis of the massif of primary measurements $(\lambda_2)_i$, while information about features of distribution of $(\lambda_2)_i$ values relating to $(\lambda_2)_{av}$ average value is practically absent. However, 60–80% of the values of secondary dendritic arm spacing have values significantly different than $(\lambda_2)_{av}$, and it should have been taken into account during analysis of conditions of forming of cast metal defects and its mechanical properties. Number of publications containing in any way this important information is rather small [1, 9, 12, 20]; they don't include descriptions of processing methods and statistical evaluations of primary data massifs, as well as any generalized data about the features of dispersion of these parameters and possible remedies of its prediction.

Presented figures 1 and 2 display the features of dispersion of primary data, relating to statistical models averaging these data. The data about λ_2 value for the alloy with 0.14% C (number of points 62, $\lambda_{av} = 237$ μm; $\lambda_{max} = 552$ μm; $\lambda_{min} = 78$ μm) [1] are described by the equation $\lambda = 146R^{-0,386}$ (the full line on the **fig. 1**, ***a***; $\sigma_\lambda = \pm 104$ μm; correlation coefficient $R = -0.946$) and form a distribution histogram for dispersion of $\Delta\lambda$ pilot data relating to regression line (see fig. 1, *b*) with root-mean-square deviation $\sigma_{\Delta\lambda} = \pm 45$ μm (dotted lines on the fig. 1, *a*) in the range 80–440 μm, what finalizes in relative dispersion about ±20%.

Dispersion of experimental data for the alloys with carbon content C = 0.08–0.70% [12] (see fig. 1, *c*) relating the partial regression lines $\lambda_2 = K_2(\tau_{LS})^{1/3}$, obtained via usage of 80–100 pilot points (multiple correlation coefficient $R = 0.975$) is characterized by $\sigma_\lambda = \pm 8.1$ μm at $\lambda_{av} = 32.7$ μm, what gives ±25%.

Microstructure of the cross section of a cylindrical sample (80 mm diam.) of 10KhGN2MB (10ХГН2МБ) steel that was cast in a mould, as well as histograms of distribution of $(\lambda_2)_i$ values (obtained on the base of investigation of these samples) are presented on the **fig. 2**. Number of measurements during investigation of dendritic structure makes 380 near the surface, 250 in the intermediate area and 150 in the axial area. Increase of local solidification time τ_{LS} from 5 to 60 s ensures elevation not only of $(\lambda_2)_{av}$, but also of dispersion of experimental data; standard deviation of this dispersion reaches ±22–26% of $(\lambda_2)_{av}$.

The presented results of metallographic investigations demonstrate the values of variation coefficient $V = \sigma_\lambda/(\lambda_2)_{av} = \pm 0.20–0.25$; these values characterize substantial dispersion of primary data. Therefore, the statistical models of dendritic structure that were previously observed (see tables 2 and 3 [36]) can be considered as not reflecting the true information about structural micro-heterogeneity, and they should be supplied with mathematical apparatus that will allow to analyze its development mechanism and to give quantitative evaluation of its real scale.

Mechanisms of appearance of local structural micro-heterogeneity. Structural micro-heterogeneity is connected with dispersion of the values of dendritic arm spacing in the scale of a separate dendrite and its nearest neighbours. It is stipulated by the fact that the process of forming the side branches has non-stationary character in the most cases (meaning thermal and concentration conditions at the tip and side surfaces of a primary trunk) and it leads to origination of a array of initial side branches $(\lambda_0)_i$ [24] that are distributed non-uniformly. Observation of dendrite growth (using transparent substances, such as ammonium chloride etc.) shows that heterogeneity of $(\lambda_0)_i$ values generates intensive competition and termination of growth for many of these

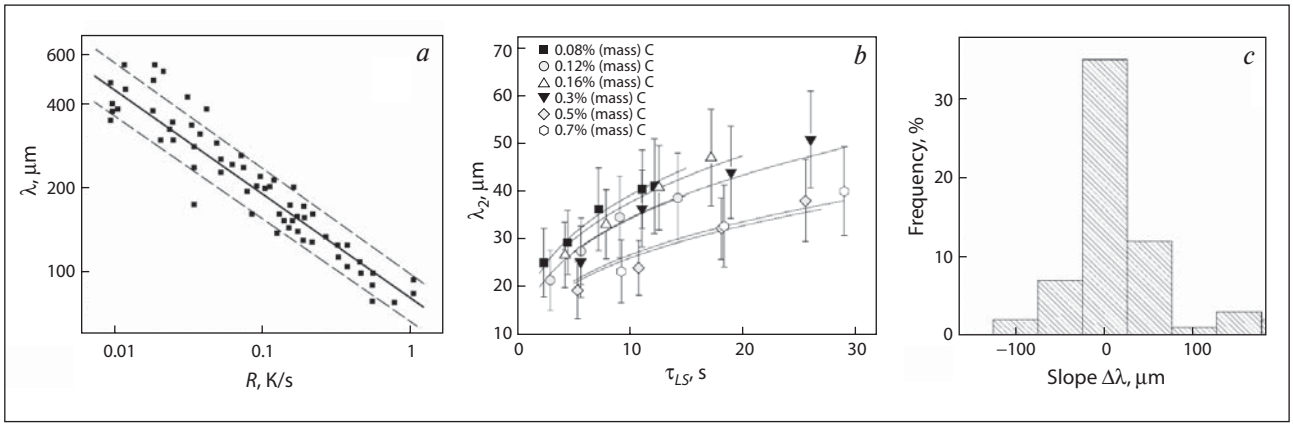

Fig. 1. Distribution of experimental data of secondary dendritic arm spacing in relation to regression lines and its depending on cooling rate *R* (*a*) [1] and solidification time (*b*) [12] in comparison with a histogram of $\Delta\lambda$ deviations (*c*), according to the data [1]

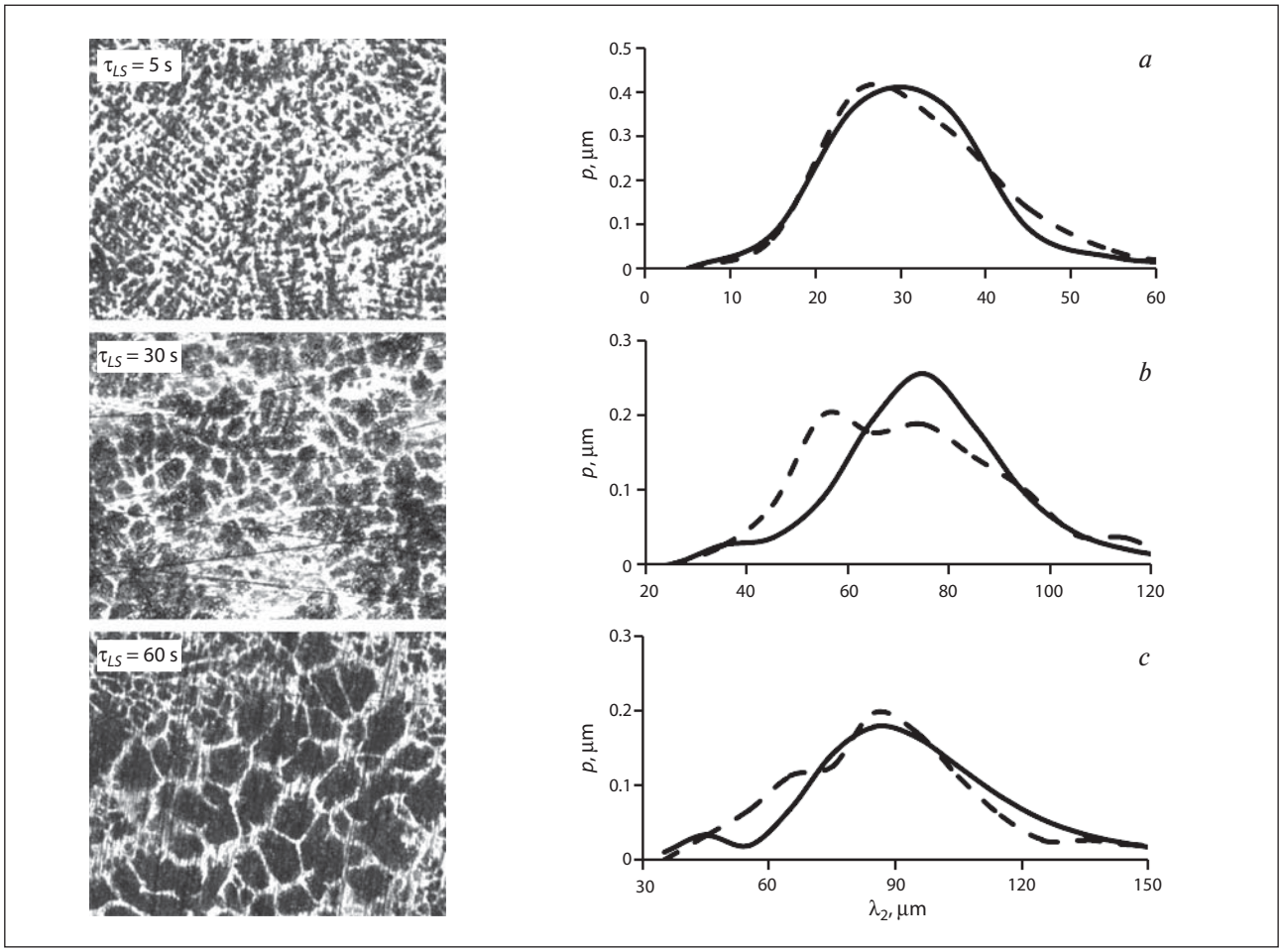

Fig. 2. Frequency distribution histograms for dendritic arm spacing in the surficial (*a*), intermediate (*b*) and axial (*c*) areas in the pilot sample, based on the results of metallographic analysis (lines) and computer-aided simulation (dotted lines) of dendritic structure (see on the left)

dendrites. It can be formulated as so-called "geometrical choosing" [24, 50], what was also noted by many researchers during quenching of metallic alloys near dendritic tips.

Afterwards complicated morphology of dendritic crystalline, characterized by curvature of interface area (different in sign and non-homogenous in value) [51], causes development of several mechanisms of diffusion coalescence of side branches, connected with their dissolution and junction under the capillary effect of Gibbs—Thomson (see fig. 1) [27, 43–47 etc.].

Usage of coalescence theory for description of the process of solid phase transition from dissolving dendritic branch *r* to a growing branch *R* allows to predict

speed of branch size variation R and r and dendritic arm spacing λ_2 depending on the conditions of crystallization, branch geometry etc. (**fig. 3**, ***b*** **and the formulas (1)–(4)**).

The equations for determination of corresponding coefficients φ [39] are presented below:

$$\varphi_I = (R/\lambda_2)^2[\ln(1 - a/R) + a/R]; \quad (1)$$
$$\varphi_{II} = (a/\lambda_2)^3[\ln(1 - r_0/a) + r_0/a + 1/2(r_0/a)^2]; \quad (2)$$
$$\varphi_{III} = 1/4[(a/\lambda_2)^2 l_0/\lambda_2]; \quad (3)$$
$$\varphi_{IV} = 1/2[(l_0/\lambda_2)^2 r_a/\lambda_2(1/(1 - r_a/R)]. \quad (4)$$

Different analytical expressions for calculation of dissolution (thickening) speed of branches during coalescence are presented in the **table**. They take into account the effect of capillary forces, morphology of dendrites (R, r и λ) and composition of liquid phase — in addition to thermal-physical factors (such as solid phase fraction m, crystallization heat Q, heat capacity c etc.) and physical chemical parameters of the alloy (such as distribution coefficient k, slope of liquidus surface p, diffusion coefficient in the melt D_L etc.).

Dependence between coalescence process and alloys composition is considered in the formulas (4), (6) and (7) of the table on the base of choosing principle for limiting alloying element (4) or for summation of additive contribution of all alloy components (6–7). It should be noted that this alternative, as well as possibility of using other approaches for multi-component alloys [52–56], still don't get any complete arguments or reliable experimental checking. The formula (6) in the table poses the most interest; it suggest choosing the suitable value of φ coefficient for one of the alternative coalescence mechanisms [39] presented on the fig. 3, *a*. Transformation of this expression (see the formula (8)) via replacement of the basic diffusion relationship — Sheil equation — allowed to give generalized description of partial diffusion in the solid phase on the base of (5) equation [36]. Evaluation of local structural microheterogeneity is realized via modeling of distribution histogram for $(\lambda_2)_i$ values using formula (8) (see the table). This histogram takes into account mutually connected passing in a row of j-th competitive mechanisms of coalescence of dendritic branches with different morphology.

Computer-aided simulation of evolution of structural micro-heterogeneity during crystallization. Analysis of the atlas of steel dendritic structures [14] and results of simulation of dendritic growth using phase field apparatus [57] allows to consider the above-presented schemes of coalescence mechanisms (fig. 3, *a*) as the basic ones in their possible separate and/or joint usage, taking into account geometrical parameters of dendritic branches (fig. 3, *b* and the formulas (1)–(4)), determining their local morphology.

In correspondence with the Monte-Carlo method [58], coalescence process was simulated for a local system from two adjacent branches (fig. 3, *b*), while their initial morphology was randomly varied. It leads to a mixed-mode evolution of $(\lambda_2)_i$ values of different systems with activation of competitive mechanisms. Multiple realization of coalescence process for substantial number of local systems allows to form a data array; collection of these data describes obtained dendritic structure using its statistical parameters: average value $(\lambda_2)_{cp}$, standard deviation σ_λ and distribution of probability density $P(\lambda_2)_i$ (frequency) in the form of histogram.

The system of equations describing non-equilibrium crystallization of multi-component alloys [24–25], presented in the previous parts of this review [36], has been used for simulation of forming of dendritic structure in the framework of a dual-level system (in meso- and micro-scale). Meso-scale was used for consideration of metal heat exchange with the environment, via solving heat balance equation. As in this case the rate of sold phase formation $dm/d\tau$ (according to equation of Kolmogorov type) depending on the value of thermal undercooling and local time of solidification τ_{LS} were calculated, i.e. taking into account non-equilibrium character of thermal processes during alloy crystallization.

Crystallization processes at micro-level have been analyzed for calculation of undercooling as well as

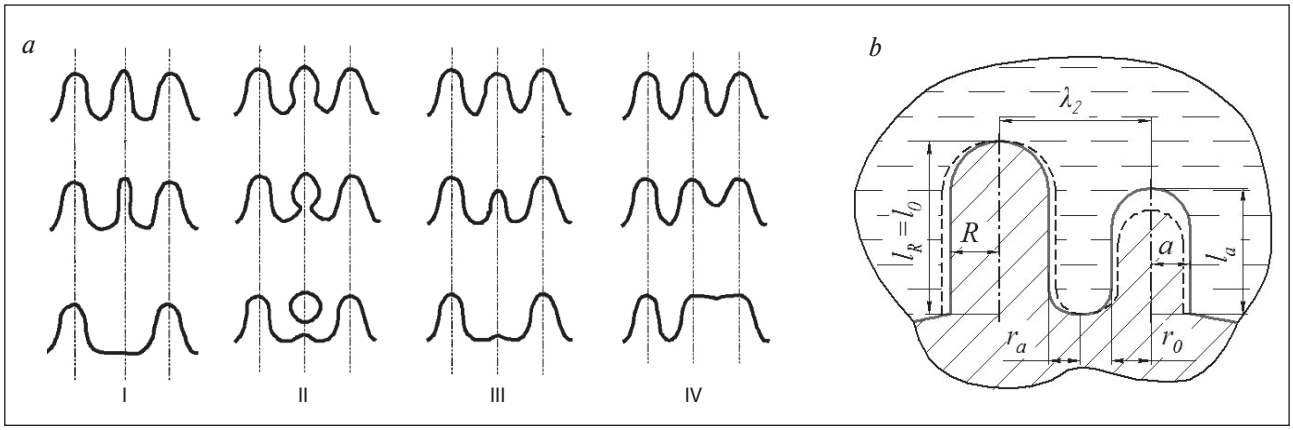

Fig. 3. Scheme of the mechanisms of coalescence of dendritic branches (*a*) and local system of branches for calculation (*c*) (I — radial dissolution, II — dissolution of base, III — axial dissolution, IV — junction of branches; R — radius of growing branch; r, r_0 — radius of dissolving branch and its base; l_0 — initial length of branches; $r_a = \lambda_2(R + a)/2$

structural micro-heterogeneity of metal. Variation of concentration of alloy components in C_L liquid phase was calculated in micro-scale according to the equation (5) [36], allowing to take into account partial suppression of diffusion in solid phase. Kinetics of growth of dendritic crystallites has been analyzed with taking their dual-stage morphological evolution into account. Forming of initial set of the values of initial dendritic arm spacing $(\lambda_0)_i$ was simulated at the I stage, including free growth and branching of equiaxial dendrites in inter-dendritic liquid phase. At the II stage, after closing of dendritic tips and stopping of their branching, modeling of solid phase formation as a result of joint radial growth of branches of cylindrical morphology and their diffusion coalescence during crystallization on intra-dendritic liquid phase has been undertaken.

When solving the reverse problem of simulation of dendritic micro-heterogeneity, the final histogram of distribution of arm spacing values (fig. 2) is the starting point. It is known by the results of microstructure investigation. Analysis of competitive character of passing of coalescence mechanisms (presented on the fig. 3, *a*) allows to determine the values of coefficients of belonging μ_j that correspond to relative value of the input of *j*-th coalescence mechanism in an integral histogram. This determination has been executed in accordance to the theory of fuzzy sets [59]. Definition of μ_j has been conducted via minimization of the sum of squares of frequency deviation *P* for calculated values $(\lambda_2)_i^P$, corresponding to *j*-th coalescence mechanism from experimental values $(\lambda_2)_i^э$:

$$F = \sum_N \left(\sum_n \mu_j P_j (\lambda_2)_i^P - P(\lambda_2)_i^э \right)^2 \rightarrow \min,$$

where *N* is a number of experimental values $(\lambda_2)_i$; *n* is a number of accounting coalescence mechanisms.

When building calculated histogram $(\lambda_2)_i^P$ for examined *j*-th coalescence mechanism, morphology of dendritic branches has been preset using basic average values [39, 44] of non-dimensional geometrical parameters (r/λ_2 and r_0/r; r_0/λ_2 and l_0/λ_2; l_0/λ_2, r_a/λ_2 and r_b/r_a; R/λ_2 relationship has been calculated based on current amount of solid phase) displayed on the fig. 3, *b* and in the formulas (1)–(4) and their probable ultimate deviations. Due to complicated character and small examination of evolution of morphology of dendritic branches in the coalescence process, these non-dimensional geometrical parameters were adopted to be constant for all period of crystallization.

Frequency of randomly chosen geometrical parameter of dendritic branches was calculated on the base of normal distribution law [35]. Possibility of pair combination of geometrical parameters was determined via multiplication of two partial probabilities; for the model IV where 3 geometrical parameters are used, the value of r_a/R relationship is adopted to be conditionally constant. Collection of frequencies obtained for randomly sample of geometrical relationships determines the frequency values for φ_j coefficients, calculated according to the formulas (1)–(4), as well as frequency for calculated values $(\lambda_2)_i^P$ in correspondence to the formula (8) in the table.

The **fig. 4** presents the typical collection of partial histograms calculated according to the described technique — with corresponding measurement ranges $(\lambda_2)_i^P$ and frequencies satisfying the conditions of independent realization of the I–IV models. Overlapping of partial distribution histograms $(\lambda_2)_i^P$ forms the wide continuous area of probable frequency values, depending on geometrical parameters of dendritic branches. These parameters are determined by the conditions of crystallization, thermal-physical and physical-chemical

Equations for evaluation of coalescence kinetics in radial dissolution of dendritic branches

№	Calculating formula	Year of publication	Reference
1	$\frac{dr}{d\tau} = \frac{\sigma p D C_0}{k_B \rho R T}\left(\frac{1}{r} - \frac{1}{R}\right)$	1956	[43]
2	$\frac{dr}{d\tau} = \frac{\sigma D T}{p \lambda L C_L (1-k)}\left(\frac{1}{r} - \frac{1}{R}\right)$	1967	[44]
3	$\lambda^2 d\lambda = \frac{9 D \Gamma}{4 C_L p (1-k) m (1-\sqrt{m})} d\tau$	1989	[45]
4	$\lambda^2 d\lambda = \min B\left(\frac{\sigma D_i^L T}{p_i (1-k_i) L_i C_i^L} d\tau\right)$	1990	[46]
5	$\lambda^2 \frac{\partial \lambda}{\partial \tau} = \frac{6 D \Gamma}{p C_L (1-k) m^{2/3} (1-m^{1/3})}$	1996	[47]
6	$\tau = \frac{L \lambda^3}{\sigma T_m} \varphi \sum \frac{p_i C_i^0 (1-k_i)(1-m)^{k_i - 1}}{D_i^L}$	1997	[39]
7	$\frac{\frac{dr}{d\tau}}{\left(\frac{1}{r} - \frac{1}{R}\right)} = \frac{\frac{\Gamma}{d}}{\sum_{(i)} \frac{p_i (1-k_i)(C_i^L)}{D_i^L}}$	1999	[48]
8	$\frac{d(\lambda^3)}{d\tau} = \Gamma \sum_{(j)} \frac{\mu_j}{\varphi_j} \frac{1}{\sum_{(i)} \frac{p_i (1-k_i) C_i^L}{D_i^L}}$	2013	[49]

Symbols: *R*, *r* — radii of dendrite branches; C_0, C_L — initial and current alloy composition; k_B — Bolzmann constant; *i* — alloy component index; φ — coefficient of model kind; *j* — coalescence mechanism index; μ — coefficient of belonging; D_L — diffusion coefficient in the melt; σ — interfacial tension; Γ — Gibbs—Thomson coefficient ($\Gamma = \sigma T/L$); *T* — absolute temperature; ρ — density; *L* — volumetric crystallization heat; *B* — geometrical factor; λ — width of secondary dendrite arm spacing; $d = \lambda - (R + r)$.

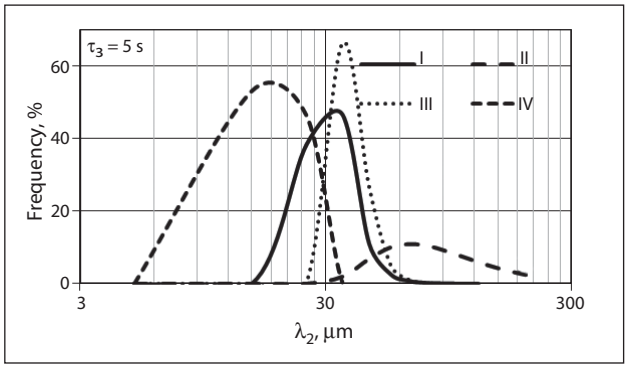

Fig. 4. Calculated distribution histograms λ_2^P for I–IV coalescence mechanisms in the surface area of a pilot sample (see fig. 2, *a*) (Preset: a/λ_2 = 0.55±0.08; r_0/a = 0.52±0.07; l_0/λ_2 = 2±0.3; r_a/λ_2 = 0.05±0.01; R/r_a =6)

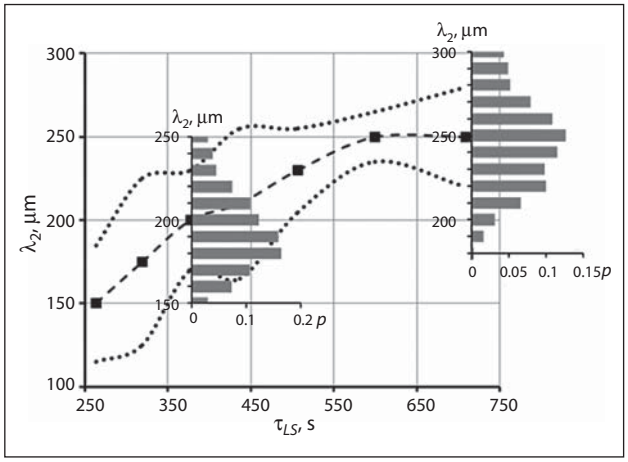

Fig. 5. Comparison of overlapped calculated histograms of probability density distribution λ_2^P with average experimental values λ_2^E (dots) and strip width $\pm\sigma_\lambda$ (dotted line) for standard deviation of experimental data [20] at different values of τ_{LS}

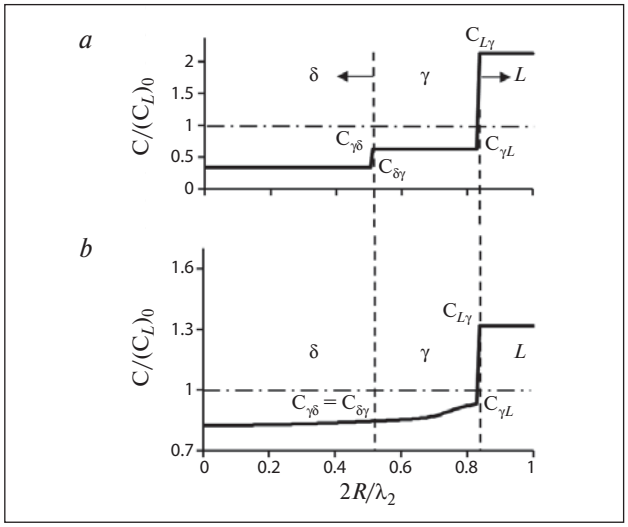

Fig. 6. Distribution of carbon (*a*) and manganese (*b*) along relative radius of dendritic branch ($2R/\lambda_2$) at the stage of peritectic transformation in comparison with equilibrium concentrations (steel 10KhGN2 (10ХГН2); τ_{LS} = 60 s; λ_2 = 100 μm; D_C^γ = 73.5·10^{-11} m^2/s; D_{Mn}^γ = 0.03·10^{-11} m^2/s; $k_C^{\gamma L}$ = 0.34; $k_{Mn}^{\gamma L}$ = 0.78)

alloy parameters, for different $(\lambda_2)_{cp}^P$ values and corresponding σ_λ range for each coalescence mechanism.

Transition from the collection of partial histograms (see fig. 4) to the joint (combined) one, describing maximally close the experimental histogram (see fig. 2), is connected with estimation of joint and competitive character of passing of different coalescence mechanisms on the base of calculations of μ_j coefficients. Obtained values of these coefficients, averaged for the period of crystallization (μ_I = 0.8–0.9; $\mu_{II} \approx \mu_{III}$ = 0.05; μ_{IV} = 0.05–0.15) [49], show that radial dissolution with unimportant input of other coalescence mechanisms plays crucial role for investigated samples.

When solving the direct problem of simulation of dendritic micro-heterogeneity via Monte-Carlo method [49], calculated array of the values of initial dendritic arm spacing $(\lambda_0)_i$, which appeared at the I stage of forming of dendritic structure, is considered as the base point. Its transformation in final distribution of the values of dendritic arm spacing $(\lambda_2)_i$ has been simulated at the next stage via analysis of kinetics of diffusion transfer of alloy components, describing by the equations suggested in [44] for a local calculated system formed by adjacent secondary branches (fig. 3, *b*). Their initial morphological parameters were preset on the base of random choice including $(\lambda_0)_i$ parameter and average values of non-dimensional geometrical parameters (r/λ_2 and r_0/r; r_0/λ_2 and l_0/λ_2; l_0/λ_2, r_a/λ_2 and r_b/r_a), as well as their probable ultimate deviations (for normal law of distribution). Duration of complete axial and/or radial dissolution of one of the branches with maximal curvature has been determined for each of more than 1,000–1,500 such calculated systems, taking into account sequential formation of solid phase and variation of branches geometry caused by this dissolution. It allows to make corresponding change in massif of values, using (8) formula in the table 1. Obtained duration

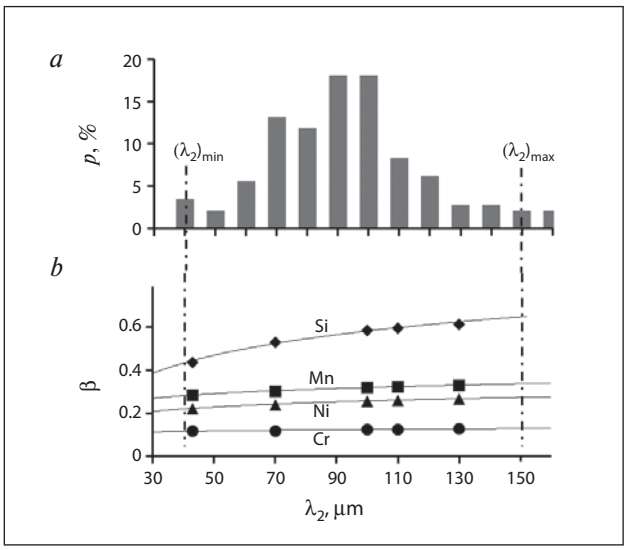

Fig. 7. Correlation between local heterogeneity of microstructure λ_2 (*a*) and degree of dendritic segregation for different components β (*b*) in the steel 10KhGN2 (10ХГН2) (τ_{LS} = 60 s)

of coalescence for that mechanisms, provided dissolution of corresponding branch, has been used in this case as local time τ_{LS} of the process.

The results of modeling of calculated distribution histograms λ_2^P, presented on the **fig. 5** in comparison with experimental data, based on the average values of λ_2^E and standard dispersion $\pm\sigma_\lambda$ for the alloy Fe — 0.07% C — 1% Mn [20], demonstrate satisfactory correlation with each other for the case of usage of non-dimensional parameters r/R = 0.7±0.2 and l_0/λ_2 = (1.9–2.2)±(1.0–2.0). Difference between calculated and experimental data λ_2^E and σ_λ is located in this case in the range 8–10 μm and 10–12 μm respectively, for variation of τ_{LS} values inside 250–720 s.

Computer-aided analysis of development of dendritic segregation, including stages of formation of δ-($L\rightarrow\delta$), γ-phase ($L\rightarrow\gamma$) and peritectic transformation ($L+\delta\rightarrow\gamma$) has been realized via numerical calculation of diffusion redistribution of the components in cross section of single-phase δ- и γ-areas and on inter-phase boundaries (based on numerical modification of Fick equation) [60–62]. Distribution of substitutional components in the layer of γ-phase, that separates the melt and δ-phase during peritectic transformation [16, 61, 62], was calculated with account of para-equilibrium on the γ/δ boundary. According to this para-equilibrium condition, carbon (intersticial component) concentration on the interface boundaries corresponds to local-equilibrium conditions (**fig. 6**, ***a***), while substitution components, due to $D_C^S >> (D_{X_i}^S)_\delta >> (D_{X_i}^S)_\gamma$ relationship, at transfer of the interface boundary inherit concentration that was formed before, on the stage of δ-phase crystallization (see fig. 6, *b*).

Chemical micro-heterogeneity $\beta = (C_{max} - C_{min})/C_0$ (**fig. 7**, ***b***), revealed via simulation, depends directly on local structural heterogeneity, presented by statistical distribution of the values of secondary dendritic arm spacing (fig. 7, *a*). The difference of concentration of steel components in a cross section of dendritic branch $(C_{max} - C_{min})_i$ is forming due to deviation of the value of distribution coefficients k_i from unity; it partially is equalized as a result of diffusion in solid phase, when coefficient of back diffusion $\sigma_i = f(D_i^S \tau_{LS}/\lambda^2)$ (see formula 5 [36]) exceeds substantially the zero value depending on local values τ_{LS} and λ_2.

Difference between $k_i^{\gamma L}$ values, determining accumulating intensity of the *i*-th component in a melt, stipulates inequality in the value of β_i parameter (fig. 7, *b*). Local heterogeneity of λ_2 value, formed during coalescence process, causes regular decrease (strengthening) of micro-segregation as a result of diffusion variation of concentration C_{min} on branch axes and C_{max} in their peripheral layers. This variation occurred under the effect of a scale factor (λ_2), which determines distance of back diffusion and value of corresponding concentration gradient. Additionally, substantial decrease of the value of diffusion coefficient (D_i^S in γ-phase) is able to eliminate dependence between micro-segregation intensity β_i and heterogeneity of dendritic structure.

The finishing part of the review, describing the less investigated problem of heterogeneity of dendritic structure in micro-scale, shows that single publications devoting anyhow to this problem and only underline lack of essential results and methodical approaches, that can reveal the main regularities of evolution transformation of the secondary dendritic branches since their origination till final state. Experimental data presented in the small amount of publications demonstrate rather substantial dispersion of the values of dendritic arm spacing, evaluating by high variation coefficient (V = 0.20–0.25). It was not reflected in the published statistical models for evaluation of secondary dendritic arm spacing (see the tables 1–3, part 1), certainly due to complicated character of this problem. Additionally, just this circumstance caused probably the above-mentioned difference in structure and parameters of the presented models operating with averaged values (λ_2); representation character of these averaged values in description of different distributions $(\lambda_2)_i$ is found to be unsatisfied.

Among the coalescence models observed in this review the most informative one is revealed; it was the base for solving the direct and reverse problems of forming the data massif on final distribution of secondary dendritic arm spacing and its statistical parameters via Monte-Carlo method. Usage of up-to-date remedies of computer tomography, possibilities of coalescence registration in micro-scale using synchrotron radiation as well as simulating remedies of phase field apparatus open the prospects of direct receiving of the important quantitative information on concealed features and evolution kinetics of dendritic structure. This information reveals typical values of geometrical parameters of dendritic structure, required for reliable forecast of complete range of the values of dendritic arm spacing, as well as mutually correlated simulation and prediction of dendritic segregation.

Conclusions

1. Joint review of publications on dendritic heterogeneity of cast steel testifies that variety and complicated character of described objects as well as conditions of their forming make the wide picture of evaluations and reveals lack of general approaches. It is directly concluded in the wide spectrum of obtained statistical models connecting averaged values of secondary dendritic arm spacing values with different thermal-physical parameters and alloys composition. Generalization of these models seems to have no prospect due to essential uncertainty of used experimental parameters and insufficient accuracy of analyzing data.

2. The radical increase in the accuracy of forecasting and analysis of the conditions of formation of the dendritic structure can be achieved through the devel-

opment and application of computer models of non-equilibrium solidification of ingots and castings (based on the use of thermo-physical and physical-chemical characteristics of the alloys, determined by their thermodynamic modeling, taking into account the rate of convective heat transfer at the front formation of dendrites), as well as via improvement of the remedies of statistical analysis of experimental data in order to provide objective evaluation of the quality of initial information and adequacy of obtained models.

3. Computer-aided analysis of evolution of the values of dendritic arm spacing on the base of calculation of their coalescence, taking into account variation of liquid phase composition in non-equilibrium crystallization, allows quantitative evaluation of the input of physical-chemical and thermal-physical factors, depending on alloys composition, on development of secondary dendritic branches. During evaluation of the effect of alloys composition on quality improvement of statistical models and provision of their adequacy, it is expedient to unify description of the pilot data on the base of polynomial form of concentrated multiplier of the regression equation. Its coefficients should be determined via the technique of orthogonal planning of experiments, to exclude the effect of pair correlation between the alloy components.

4. Using Monte Carlo method allows to solve the problem about final distribution of the local values of the secondary dendritic arm spacing and their statistical parameters characterizing heterogeneity of cast dendritic structure. These parameters characterize microheterogeneity of a cast dendritic structure. Accumulation and generalization of the data about morphological (geometrical) dendritic parameters and their evolution ion competitive realization of different coalescence mechanisms is the important task for reliable predicting of these parameters. System analysis of the redistribution of steel components during crystallization shows that the local development of dendritic segregation is directly dependent on the structural micro-inhomogeneity and features of diffusion conditions in the solid phase and at interfaces.

REFERENCES (Part 3)

43. *Chernov A. A.* Kristallografiya — Crystallography Reports. 1956. Vol. 1, Iss. 5. pp. 589–593.
44. *Kattamis T. Z., Coughlin J. C., Flemings M. C.* Influence of coarsening on dendrite arm spacing of aluminium-copper alloys. Transactions of AIME. 1967. Vol. 239, No. 10. pp. 1504–1511.
45. *Mortensen A.* On the rate of dendrite arm coarsening. Metallurgical and Materials Transactions. 1991. Vol. 22A, No. 2. pp. 569–574.
46. *Roosz A., Exner H. E.* Numerical modeling of dendritic solidification in aluminium-rich Al-Cu-Mg alloys. Acta Metallurgica et Materialia. 1990. Vol. 38, No. 2. pp. 375–80.
47. *Nastac L., Stefanescu D. M.* Macrotransport — solidification kinetics modeling of equiaxed dendritic growth: Part. 1. Model development and discussion. Metallurgical and Materials Transactions. 1996. Vol. 27A, No. 12. pp. 4061–4074.
48. *Rappaz M., Boettinger W. J.* On solidification of multicomponent alloys with unequal liquid diffusion coefficient. Acta Materialia. 1999. Vol. 47, No. 11. pp. 3205–3219.
49. *Emelyanov K. I., Golod V. M.* Liteyshchik Rossii — Russian founder. 2013. No. 2. pp. 28–33.
50. *Kolmogorov A. N.* Doklady Akademii Nauk SSSR — Reports of USSR Academy of Sciences. 1949. Vol. 65, No. 5. pp. 681–684.
51. *Feijoo D., Exner H.* Surface curvature distribution of growing dendrite crystals. Journal of Crystal Growth. 1991. Vol. 113, No. 3–4. pp. 449–455
52. *Tensi H. M., Fuchs H.* Dendritenarmvegröberung bei binären und ternären Aluminium-Legierungen. Zeitscrift für metallkunde. 1983. Bd. 74, H. 6. ss. 351–357.
53. *Ronto V., Roosz A.* Numerical simulation of dendrite arm coarsening in case of ternary Al alloys. Materials Science Forum. 2003. Vol. 414–415. pp. 483–490.
54. *Ilinskiy V. A., Kostyleva L. V., Goremykina S. S.* Izvestiya vuzov. Chernaya metallurgiya – Proceedings of universities. Ferrous metallurgy. 2007. No. 1. pp. 16–19.
55. *Ilinskiy V. A., Kostyleva L. V., Goremykina S. S.* et al. Metally — Metals. 2005. No. 6. pp. 66–70.
56. *Goremykina S. S., Kostyleva L. V., Ilinskiy V. A.* Metallurgiya mashinostroeniya — Metallurgy of Machinery Building. 2005. No. 5. pp. 28–30.
57. *Boettinger W. J.* et al. Phase-field simulation of solidification. Annual Review of Materials Research. 2002. Vol. 32. pp. 163–194.
58. *Sobol I. M.* Chislennye metody Monte-Karlo (Numerical methods of Monte-Carlo). Moscow : Nauka, 1973. 312 p.
59. *Zade L. A.* Ponyatie lingvisticheskoy peremennoy i ego primenenie k prinyatiyu priblizhennykh resheniy (Concept of linguistic variable and its application to approximate solutions making). Moscow : Mir, 1976. 163 p.
60. *Ueshima Y.* et al. Analysis of solute distribution in dendrites of carbon steel with δ/γ transformation during solidification. Metall. Trans., 1986, v. 17B, p. 845–859.
61. *Thuinet L., Combeau H., Lesoult G.* Microsegregation in steels during dendritic columnar growth and peritectic reaction. Part II: Modelling and numerical simulation. Comparison with experimental results. Mater. Sci. Forum, 2006, v. 508, p. 367–372.
62. *Natsume Y., Shimamoto M., Ishida H.* Numerical modeling of microsegregation for Fe-base multicomponent alloys with peritectic transformation coupled with thermodynamic calculations. ISIJ Int., 2010, v. 50, No. 12, 1867–1874.